High-temperature superconductivity below 100 GPa in ternary C-based hydride MC_2H_8 with molecular crystal characteristics (M = Na, K, Mg, Al, and Ga)

Meng-Jing Jiang,[1,2] Yu-Long Hai,[1,2] Hui-Li Tian,[1,2] Han-Bin Ding,[1,2] Yu-Jie Feng,[1,2] Chun-Lei Yang,[1,3,*]
Xiao-Jia Chen ®,[4,5,†] and Guo-Hua Zhong ®[1,3,‡]

[1]*Shenzhen Institute of Advanced Technology, Chinese Academy of Sciences, Shenzhen 518055, China*
[2]*Nano Science and Technology Institute, University of Science and Technology of China, Suzhou 215123, China*
[3]*University of Chinese Academy of Sciences, Beijing 100049, China*
[4]*School of Science, Harbin Institute of Technology, Shenzhen 518055, China*
[5]*Center for High Pressure Science and Technology Advanced Research, Shanghai 201203, China*

To explore the high-temperature superconductivity of hydrogen-rich compounds at low pressures, we have investigated the crystal structures, electronic and dynamical properties, electron-phonon interactions, and possible superconductivity of the ternary hydride MC_2H_8 (M = Na, K, Mg, Al, and Ga) in the low-pressure range of 0–100 GPa based on the first-principles calculations. The results show that there is no imaginary frequency in phonon spectra for MC_2H_8 at selected pressures which indicates that MC_2H_8 is dynamically stable. Furthermore, according to the Eliashberg spectral function under pressures, MC_2H_8 is predicted to be superconducting at low pressure. Especially, the superconducting critical temperature (T_c) of MgC_2H_8 is higher than 55 K at 40 GPa and the T_c in AlC_2H_8 reaches 67 K at 80 GPa. Electronic and phonon states and the electron-phonon interactions show that H has a considerable contribution to this ternary hydride superconductor and suggest that increasing the contribution of H to total electron-phonon coupling is a way to design materials with high T_c. Our study shows that it is one of the feasible routes to explore the low-pressure and high-temperature superconductivity in ternary carbon-based hydrides.

I. INTRODUCTION

Remarkable success has been achieved in exploring high- and room-temperature superconductivity in binary hydrides. The superconducting transition temperature (T_c) observed in the experiment has approached or exceeded zero °C. For example, T_c of 203 K was observed in sulfur hydride at 155 GPa [1], 250–260 K was observed in lanthanum hydride at 180–170 GPa [2,3], 262 K in yttrium superhydride at 182 GPa [4], 243 K in yttrium hydride at 201 GPa [5], and 224 K in YH_6 at 166 GPa [6]. However, a problem that can not be ignored is that the pressure conditions required to produce such a superconducting critical temperature are very harsh. The binary hydrides mentioned above usually exist stably and exhibit high-temperature superconductivity at a high pressure above 150 GPa. Such harsh experimental conditions will limit the application of hydride superconductors. Hence, it is very necessary to explore hydride superconductors with high-T_c value at low pressures such as below 100 GPa.

Compared with binary hydrides, ternary hydrides, especially MA_xH_y-type ternary hydrides in which M and A represent metal and main group nonmetallic elements, have been considered as the promising candidates of high-T_c

low-pressure superconductors since the superconductivity of $T_c \sim 150$ K was predicted at 12 GPa in KB_2H_8 [7]. Focused on pressure equal to or lower than 100 GPa, many important theoretical predictions on MA_xH_y have been carried out [7–18]. In particular, when A is carbon element, the hydrocarbon sublattice can been formed in the crystal MC_xH_y, which is the significant structure characteristics in materials and is also one of the most desirable structures to obtain superconductivity. When the quasimolecule form of methane (CH_4) was formed in MC_xH_y, Tian *et al.* reported that T_c in $MgCH_4$ with $P4/nmm$ symmetry reaches 84 K at 75 GPa [8]. However, the stability of $MgCH_4$ could not be checked. Subsequently, some of the authors of this paper predicted the stable structures of KCH_4 [10], $BeCH_4$ [11], $Li_x(CH_4)_{1-x}$ [12], and $Ba_x(CH_4)_{1-x}$ [18] with containing quasimolecule of CH_4, and also suggested that the systems can exhibit metallic behavior and superconductivity at low pressures such as 5 and 10 GPa. For example, T_c of $Amm2 - Ba(CH_4)_3$ exceeds 24 K at 20 GPa, and increases to 43.7 K at 90 GPa [18]. Those studies show that ternary hydride MC_xH_y with molecular crystal characteristics can be metallized at low pressures and exhibits the high-temperature superconductivity.

From the reported results, however, the T_c of ternary hydride is still lower than that of binary hydride, although the low-pressure superconductivity is realized. Hence, improving the T_c, more MC_xH_y-type ternary hydride superconductors need to be explored, or more studies on MC_xH_y are needed. In this work, therefore, we choose MC_2H_8 ternary

*cl.yang@siat.ac.cn
†xjchen@hpstar.ac.cn
‡gh.zhong@siat.ac.cn

hydride with CH_4 molecular characteristics to explore the low-pressure and high-temperature superconductivity, based on the first-principles calculations. MC_2H_8 can be regarded as a metal-doped CH_4 molecular solid, with the $Fm\bar{3}m$ space group. At the same time, methane is the simplest of saturated hydrocarbons and one of the most abundant organic molecules in the universe. It is of great significance to study the metallization and superconductivity of methane solid. Differing from $P4/nmm$ of $MgCH_4$ [8], $P2_1/m$ of KCH_4 [10], $P1$ of $BeCH_4$ [11], $P2_1$ of $Li(CH_4)_4$ [12], and $Amm2$ of $Ba(CH_4)_3$ [18], the doping concentration of metal in MC_2H_8 is reduced by half. Here, investigating the crystal structures, electronic states, and electron-phonon interactions of MC_2H_8 (M = Na, K, Mg, Al, and Ga) at the low-pressure range of 0–100 GPa, we predict that T_c of MgC_2H_8 is higher than 55 K at 40 GPa and T_c of AlC_2H_8 can reach 67 K at 80 GPa. The higher superconducting transition temperature is obtained in MC_2H_8 ternary hydride.

II. COMPUTATIONAL DETAILS

In this work, we referred to the structural feature of KB_2H_8 [7] and constructed the crystal structure of MC_2H_8 (M = Na, K, Mg, Al, and Ga). Selected typical pressure points of 0, 20, 40, 60, and 80 GPa, we performed the structural optimizations and self-consistent energy calculation by using Vienna *ab initio* simulation package (VASP) [19,20] based on the exchange-correlation functional of generalized gradient approximation (GGA) in version of Perdew-Burke-Ernzerhof (PBE) [21] and projector augmented wave pseudopotentials [22]. The plane-wave cutoff energy was set as 600 eV. In the optimization process, convergence thresholds were set as 10^{-5} eV in energy and 10^{-3} eV/Å in force. The k-point interval distribution of Monkhorst-Pack was 0.04 Å^{-1} for structural optimization and 0.02 Å^{-1} for self-consistent energy calculation, respectively.

The phonon frequencies and electron-phonon interactions were calculated by employing the QUANTUM ESPRESSO package (QE) [23,24]. The cutoff energies of 80 Ry were used for wave functions. In both VASP and QE codes, the same functional was selected. Forces and stresses for the converged structures were optimized and checked to be within the error allowance of the VASP and QE codes. Based on the calculated Eliashberg spectral function [$\alpha^2F(\omega)$]

$$\alpha^2F(\omega) = \frac{1}{2\pi N(0)} \sum_{Qv} \frac{\gamma_{Qv}}{\omega_{Qv}} \delta(\omega - \omega_{Qv}), \quad (1)$$

the electron-phonon coupling constant (λ) is obtained:

$$\lambda = 2 \int_0^\infty \frac{\alpha^2F(\omega)}{\omega} d\omega. \quad (2)$$

Furthermore, T_c was estimated by the Allen-Dynes–corrected McMillan equation [25], expressed as

$$T_c = f_1 f_2 \frac{\omega_{\log}}{1.2} \exp\left[-\frac{1.04(1+\lambda)}{\lambda - \mu^*(1+0.62\lambda)} \right]. \quad (3)$$

In the modified McMillan equation, $\mu^\star$ represents the Coulomb pseudopotential which was taken as 0.1 in our calculations. $\omega_{\log}$ is the logarithmic average of phonon frequency:

$$\omega_{\log} = \exp\left[\frac{2}{\lambda} \int_0^\infty \frac{\alpha^2F(\omega)\log(\omega)}{\omega} d\omega) \right]. \quad (4)$$

The factor $f_1 f_2$ depends on the λ, $\mu^\star$, $\omega_{\log}$, and mean-square frequency ($\overline{\omega_2}$) [25].

III. RESULTS AND DISCUSSION

Starting from the optimized crystal structures, the enthalpy of formation of MC_2H_8 is compared with several possible decomposition enthalpies. The structures of each decomposition product are taken from previous studies: Na ($P6_3/mmc$ and $Fm\bar{3}m$) [26,27], NaC ($Immm$) [28], K ($P6_3/mmc$, $Fm\bar{3}m$, and $Im\bar{3}m$) [27,29,30], KC_2 ($P4/nmm$) [31], KH ($Fm\bar{3}m$) [32], KH_3 ($I4/mmm$) [27], KCH_4 ($R3m$ and $P2_1/m$) [10], Mg ($Im\bar{3}m$) [33], MgC_2 ($P4_2/mnm$) [34], MgH_2 ($Fm\bar{3}m$) [35], $MgCH_4$ ($Pban$ and $P4/nmm$) [8], Al ($Fm\bar{3}m$) [36], AlH_3 ($Fd\bar{3}m$)[37], Al_4C_3 ($R\bar{3}m$)[38], Ga ($Cmcm$ and $I4/mmm$) [39,40], GaC (($P6_3mc$) [27], GaH ($P6_3mc$) [27], GaH_3 ($I4/mmm$) [27], C ($Fmmm$ and $P6_3/mmc$) [27], CH_2 ($Cmcm$) [41], CH_4 ($P2_1/c$) [41], and H_2 ($P6_3/m$) [42]. Calculated enthalpy difference versus pressure for MC_2H_8 is shown in Fig. 1. As shown in Figs. 1(a) and 1(e), when the pressure is larger than 20 GPa, the enthalpy values of NaC_2H_8 and GaC_2H_8 are lower than those of their possible decomposition forms, which means that NaC_2H_8 and GaC_2H_8 are thermodynamically stable above 20 GPa. Comparing with the possible decomposition enthalpies, we can see that both KC_2H_8 and AlC_2H_8 can stably exist in the whole pressure range considered [Figs. 1(b) and 1(d)], while MgC_2H_8 is thermodynamically stable only below 40 GPa. Moreover, for MC_2H_8 (M = Na, K, Mg, Al, and Ga), the metallization and dynamical stability were also examined in the pressure range of 0–100 GPa, the results are presented in Figs. S1– S10 of the Supplemental Material (SM) [43]. If no imaginary frequency is observed, the system is dynamically stable.

When MC_2H_8 satisfying the conditions of metallization and thermodynamic and dynamical stabilities, we calculated its electron-phonon coupling constant λ and logarithmic average of phonon frequency $\omega_{\log}$ and estimated its superconducting critical temperature T_c. Figure 2 shows the dependence of T_c, λ, and $\omega_{\log}$ on pressure for MC_2H_8 (M = Na, K, Mg, Al, and Ga). As reflected in Eq. (3), T_c is competitively determined by λ and $\omega_{\log}$. Under the symmetry of $Fm\bar{3}m$ space group, it was found that the monovalent metal-doped cases NaC_2H_8 and KC_2H_8 lead to the relatively low-λ and -T_c values, which are less than 0.7 and 30 K in the pressure range of 0–100 GPa, respectively. NaC_2H_8 and KC_2H_8 are comparable with $Li(CH_4)_4$ [12] and KCH_4 [10] in the superconductivity. And KC_2H_8 can only stabilize above 50 GPa. Interestingly, MgC_2H_8, AlC_2H_8, and $GaKC_2H_8$ exhibit the high superconductivity below 50 GPa. For example, the T_c of MgC_2H_8 rapidly increases with the increase of pressure and reaches 55 K at 40 GPa, though it is not stable above 50 GPa. Both AlC_2H_8 and $GaKC_2H_8$ are stable and superconductive in the considered pressure range of 0–100 GPa. These two systems have the T_c higher than 50 K below 60 GPa, however, the T_c of AlC_2H_8 continues to increase with the pressure and reaches 67 K at 80 GPa, while the T_c of GaC_2H_8 decreases
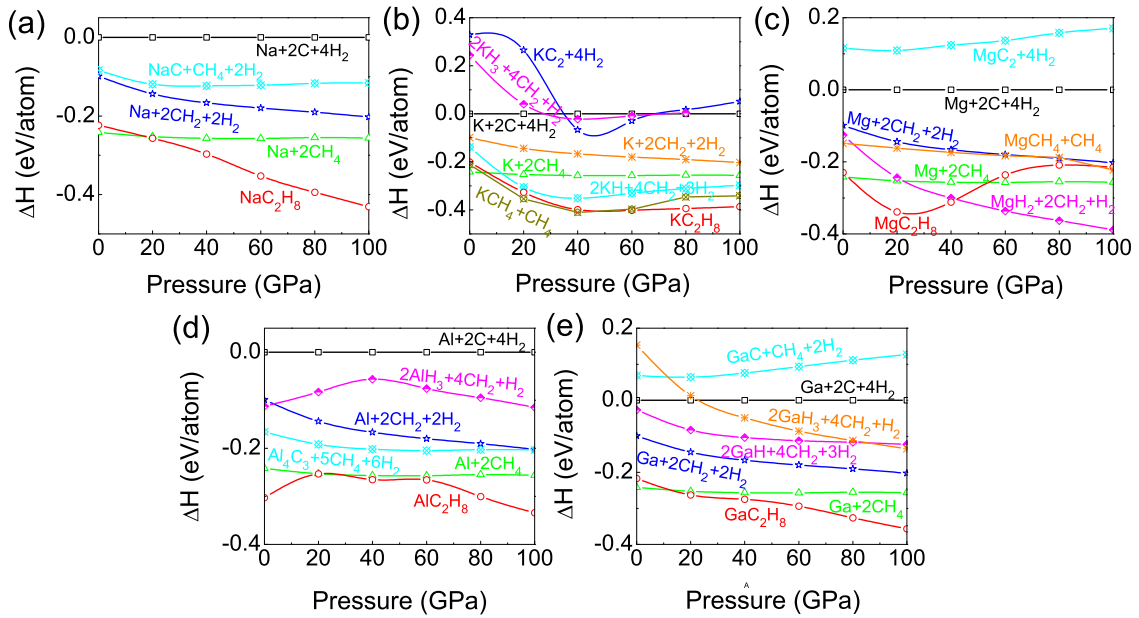
FIG. 1. Calculated enthalpy difference versus pressure for MC_2H_8, referenced to the decomposition enthalpy into element phase of $M + 2C + 4H_2$. The other possible decomposition enthalpies were considered. (a)–(e) Correspond to NaC_2H_8, KC_2H_8, MgC_2H_8, AlC_2H_8, and GaC_2H_8, respectively.

with the pressure after 60 GPa. Comparing with our previous studies on $Li(CH_4)_4$ [12], KCH_4 [10], $BeCH_4$ [11], and $Ba(CH_4)_3$ [18], MC_2H_8 creates the bigger ω_{log} value at the same pressure, which is just reason of that it has higher T_c. However, the λ of MC_2H_8 is less than those of KB_2H_8 [7] and $LaBH_8$ [13,14], though MC_2H_8 has bigger ω_{log}. In addition, comparing with the λ close to 2 or greater than 2 in binary hydride, the λ of MC_2H_8 is relatively low and difficult to exceed 1. Hence, further improving the electron-phonon interaction is the main means to improve the T_c of MC_2H_8. But, it is worth noting that the T_c of MC_2H_8 does not increase or decrease monotonically with the increase of pressure. From Eq. (3), T_c is determined by λ and ω_{log}, and both of them are related to $\alpha^2 F(\omega)$. Namely, the superconductivity is determined by both electronic and phonon states. Although the phonon frequency changes gradually with the increase of pressure as shown in Figs. S6– S10 [43], the value of density of states (DOS) at Fermi level does not vary monotonically with the increase of pressure from the electronic structures shown in Figs. S1– S5 [43], which leads to the nonmonotonic change of T_c of MC_2H_8. Next, we will understand the MC_2H_8 superconductor from the perspective of crystal structure, electronic characteristics, and electron-phonon coupling in the cases of MgC_2H_8 and AlC_2H_8.

MC_2H_8 has the $Fm\bar{3}m$ symmetry which is a common space group in hydrides with high T_c. M, C, and H atoms occupy the $4a$ (0.000, 0.000, 0.000), $8c$ (0.250, 0.250, 0.250), and $32f$ (0.360 ± u, 0.360 ± u, 0.360 ± u) Wyckoff positions, respectively. The u value is affected by pressure and doped metal. The crystal structures in the cases of MgC_2H_8 and AlC_2H_8 are shown in Figs. 3(a) and 4(a), respectively. The CH_4 tetrahedrons are formed between C and H atoms, namely, methane quasimolecules, and there are eight CH_4 molecules in the unit cell of MC_2H_8. From electron localization function

(ELF) shown in Figs. 3(b) and 4(b), the bonding between different CH_4 quasimolecules is neither the covalent bond nor the ionic bond, but a weak intermolecular force. During pressurization, MC_2H_8 has always maintained the molecular crystal characteristics, and the intermolecular interaction between two CH_4 quasimolecules increases. In order to evaluate whether CH_4 will rotate in the system, we designed a hypothetical structure so that CH_4 quasimolecule has an arbitrary rotation. In the case of MgC_2H_8 (at 40 GPa) and AlC_2H_8 (at 80 GPa) as shown in Fig. S11 [43], it was found that the total energy increases when the CH_4 molecules rotate. After rotating, as shown in Table S1 [43], the total energy increased by 0.11 and 0.34 eV/f.u. for MgC_2H_8 (at 40 GPa) and AlC_2H_8 (at 80 GPa), respectively. This indicates that CH_4 molecules are not easy to rotate, especially under high pressure.

The C-H bonding lengths in MgC_2H_8 (at 40 GPa) and AlC_2H_8 (at 80 GPa) are, respectively, 1.124 and 1.115 Å, which are less than 1.227 Å of B-H bond in KB_2H_8 at 12 GPa [7] and 1.33 Å of B-H bond in $LaBH_8$ at 150 GPa [14], obviously shorter than the 1.546 Å of S-H bond in in SH_3 at 150 GPa [44]. From ELFs shown in Figs. 3(b) and Fig. 4(b), a strong polar covalent bond is formed between C and H atoms, which is the main reason for the stable existence of CH_4 at low pressure. In addition, the charge transfer occurs from metal atom to CH_4 molecules. Comparing MgC_2H_8 (at 40 GPa) with AlC_2H_8 (at 80 GPa), the ionic character between metal and CH_4 is slightly different, which may depend on the valence state and electronegativity of the metal. The charge transfer was examined by calculating Bader charge [45,46]. Table S2 [43] presents the transferred charge from M to CH_4 at different pressure for MC_2H_8. The transferred charges from M to CH_4 are 1.52 e/Mg and 1.65 e/Al in MgC_2H_8 (at 40 GPa) and AlC_2H_8 (at 80 GPa), respectively. In fact, the charge is transferred to C atoms from metal. In NaC_2H_8, KC_2H_8, and
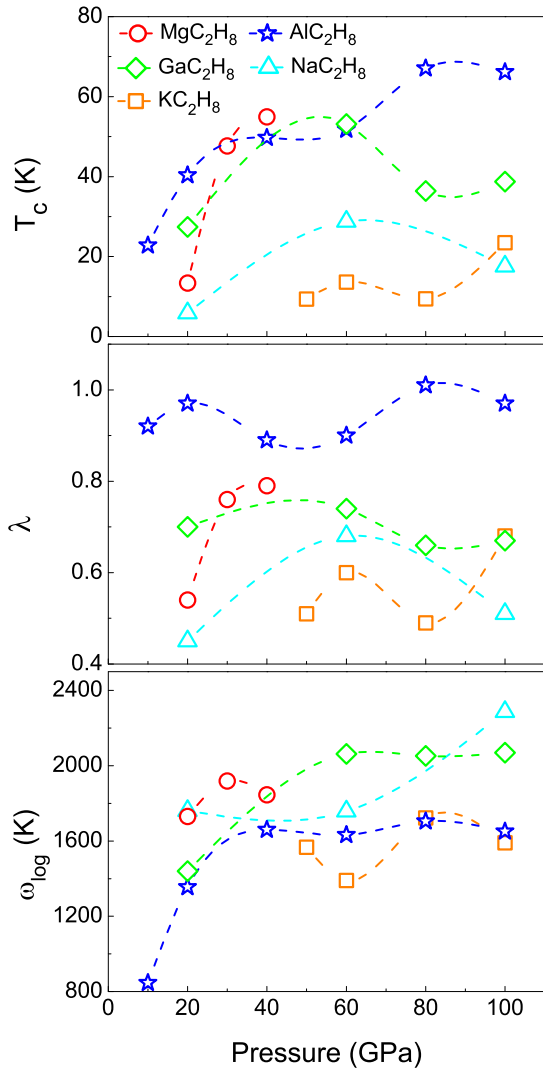
FIG. 2. The calculated superconducting critical temperature T_c, electron-phonon coupling constant λ, and logarithmic average of phonon frequency $\omega_{\log}$ for NaC_2H_8, KC_2H_8, MgC_2H_8, AlC_2H_8, and GaC_2H_8 change with the pressure.

GaC_2H_8, the relatively less charge is also transferred to C atoms, which are 0.74 e/Na at 60 GPa, 0.69 e/Na at 100 GPa, and 0.66 e/Ga at 60 GPa, respectively. This difference in charge transfer leads to differences in electronic states.

Methane solid is a wide-gap semiconductor with a band gap of 7.7 eV at ambient pressure [47], and the band gap of methane will not close until 500 GPa at room temperature [41,47–49]. However, previous theoretical studies have predicted that the metal-doped methane can become to metal at low pressure [8,10–12,18]. In this work, we further confirmed this point. Due to the charge transfer from metal to CH_4 molecules, MC_2H_8 realizes the metallization at the considered low-pressure range of 10–100 GPa. For MgC_2H_8 at 40 GPa as shown in Figs. 3(c) and 3(d), four bands cross the Fermi level to form the complex Fermi-surface (FS) sheets such as holelike FS around the L point and electronlike FS around the W and Γ points. With the same space group, AlC_2H_8 at 80 GPa has four bands crossing the Fermi level as shown in Fig. 4(c). Due to the metallization from charge transfer, there

is the similar character between MgC_2H_8 and AlC_2H_8, which are the increase of Fermi level caused by charge transfer. Only because of the different electronegativity and valence states of metals, the amount of charge transfer is different which results in that the shift of Fermi level is different. The relative movement of the energy bands leads to the change of the size and shape of the electronlike and holelike FSs. Hence, the shape of FSs is different between MgC_2H_8 and AlC_2H_8. At the same time, the pressure will also cause the shift of the Fermi level, resulting in the change of the number of FSs. For example, at 20 GPa, there are two bands crossing the Fermi level and forming the FSs in MgC_2H_8 (Fig. S13 [43]), while three bands cross the Fermi level and form the FSs in AlC_2H_8 (Fig. S14 [43]). In addition, the pressure will expand the electronic state, so the energy gap will decrease with the increase of pressure. For example, an energy gap of 1.2 eV around -5 eV in Mg_2H_8 at 40 GPa will disappear in Al_2H_8 at 80 GPa, as shown in Figs. 3(c) and Fig. 4(c).

From the projected DOS on atomic orbitals, the electronic states near the Fermi level mainly come from C-2p, but the contribution of Mg-s, p (Al-s, p) and H-s to FS is also considerable. Focusing on the DOS values at Fermi level, the results of MC_2H_8 are presented in Table S3 [43]. As a result, the DOS values at Fermi level reach 0.78 and 0.91 states/eV/f.u. in MgC_2H_8 at 40 GPa and AlC_2H_8 at 80 GPa, respectively. This result of density of electronic states at Fermi level is larger than 0.4 states/eV/f.u. of SH_3 at 200 GPa [50], 0.52 states/eV of $LaBH_8$ at 50 GPa [13], 0.60 states/eV of KB_2H_8 at 12 GPa [7], and 0.50 states/eV/f.u. of $Li(CH_4)_4$ at 100 GPa [12], comparable with 0.75 states/eV/f.u. of LaH_{10} at 250 GPa [51], 0.87 states/eV/f.u. of $MgCH_4$ at 90 GPa [8], and 0.90 states/eV/f.u. of $BeCH_4$ at 80 GPa [11], slightly less than 1.57 states/eV/f.u. of KCH_4 at 80 GPa [10] and 1.44 states/eV/f.u. of $Ba(CH_4)_3$ at 90 GPa [18]. With regard to pressure effect, the DOS values at Fermi level for MgC_2H_8 and AlC_2H_8 are different at different pressures. As shown in Fig. S3 [43], the DOS value at Fermi level at the pressure with the highest T_c is not the largest for MgC_2H_8. The similar situation was also observed in AlC_2H_8 as shown in Fig. S4 [43]. In addition, as shown in Table S1 and Fig. S12 [43], at low pressure, the DOS value at Fermi level changes obviously due to the rotation of CH_4 molecules, which is related to the easier rotation of molecules at low pressure. On the contrary, at high pressure, the DOS value at Fermi level caused by molecular rotation changes little. Other metals such as Na-, K-, and Ga-doped cases, the electronic DOSs exhibit the metallic feature, and the relative big DOS values at Fermi level are obtained in NaC_2H_8, KC_2H_8, and GaC_2H_8 (see Figs. S1, S2, and S5 [43]). The phonon structures including phonon spectra and phonon density of states (PhDOS) shown in Fig. 5 present the difference between MgC_2H_8 at 40 GPa and AlC_2H_8 at 80 GPa. Comparing with the Raman spectrum of pure CH_4 solid [52–58], the phonon frequencies of MgC_2H_8 and AlC_2H_8 at gamma are reduced in the high-frequency region, which is mainly because the vibration frequency of the system is weakened after metal doping to form crystals. Although metal doping forms a new crystal structure, the vibrational modes of atoms and molecules still retain some characteristics. For MgC_2H_8 at 40 GPa, referring to the Raman modes of CH_4 solid [52–58], the phonon spectra MgC_2H_8 can be divided
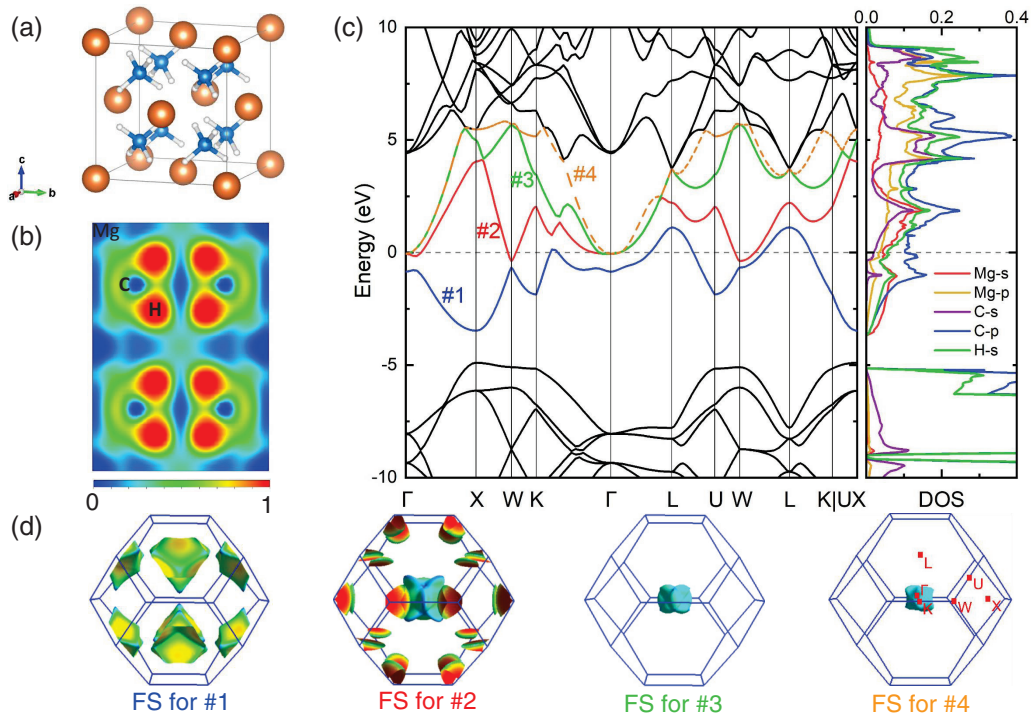
FIG. 3. (a) Optimized crystal structure, (b) the two-dimensional electron localization function in (101) plane, (c) the electronic band structures and projected density of states (DOS) on atomic orbitals where the Fermi level is set as zero, (d) the Fermi-surface features corresponding to four energy bands crossing the Fermi level of MgC_2H_8 at 40 GPa.
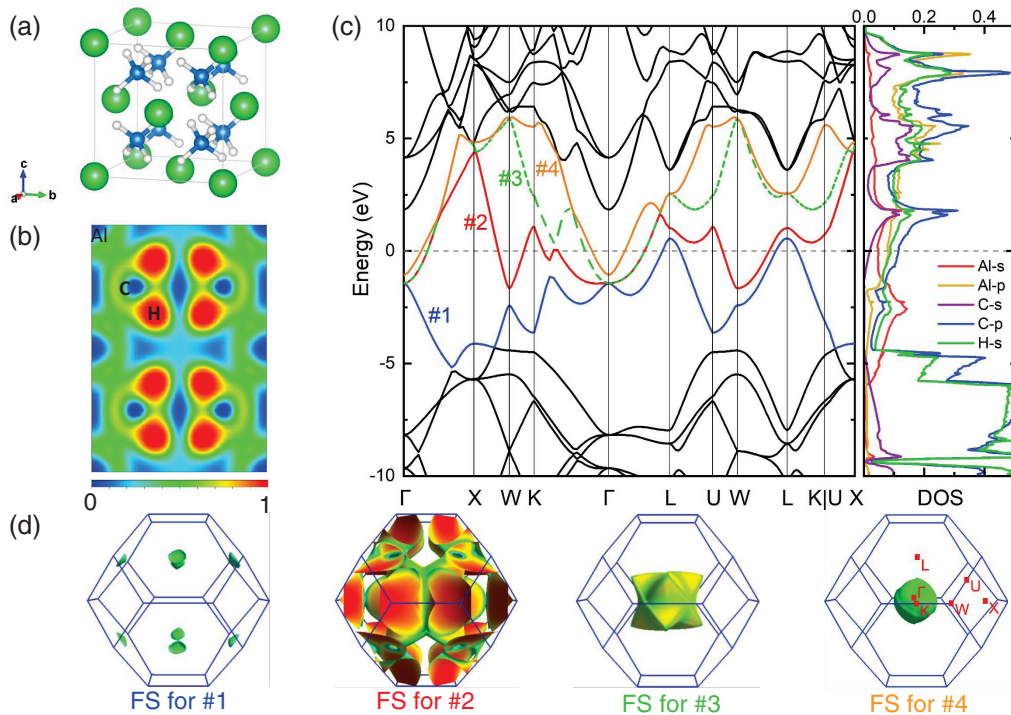
FIG. 4. (a) Optimized crystal structure, (b) the two-dimensional electron localization function in (101) plane, (c) the electronic band structures and projected density of states (DOS) on atomic orbitals where the Fermi level is set as zero, (d) the Fermi-surface features corresponding to four energy bands crossing the Fermi level of AlC_2H_8 at 80 GPa.
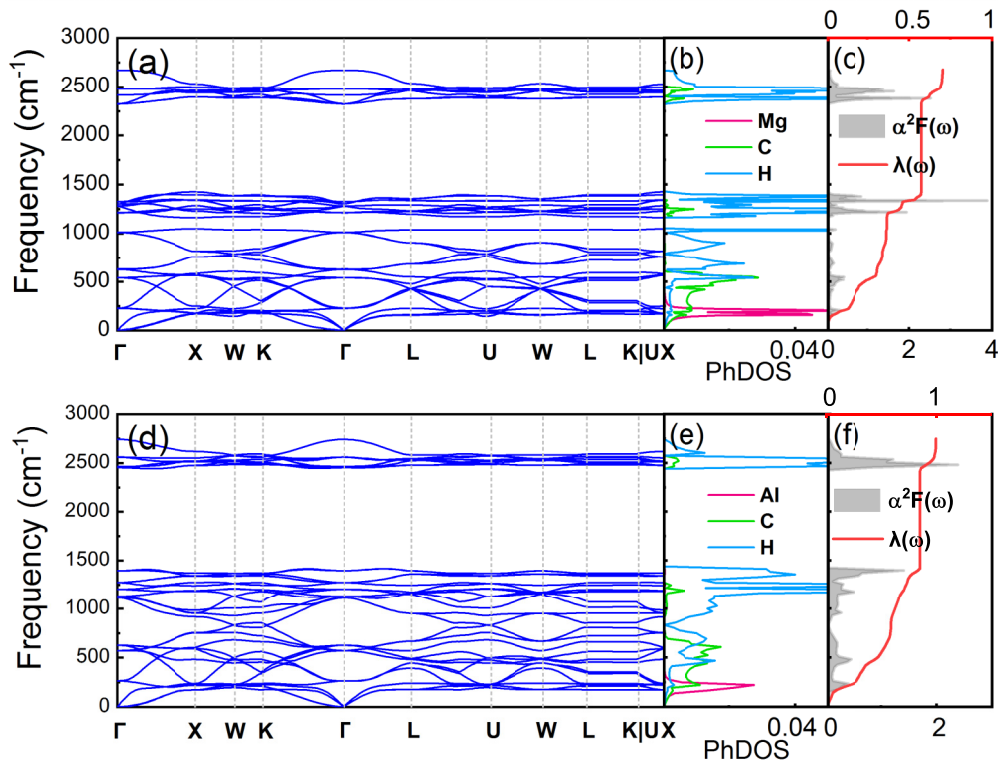
FIG. 5. The calculated (a) phonon spectra, (b) phonon density of states (PhDOS), (c) Eliashberg spectral function $\alpha^2 F(\omega)$, and electron-phonon coupling integral $\lambda(\omega)$ of MgC_2H_8 at 40 GPa. And the calculated (d) phonon spectra, (e) phonon density of states (PhDOS), and (f) Eliashberg spectral function $\alpha^2 F(\omega)$, and electron-phonon coupling integral $\lambda(\omega)$ of AlC_2H_8 at 80 GPa.

into three parts according to the contribution of elements. In H-dominated region, the high-frequency modes in the range of 2346–2644 cm^{-1} mainly come from the stretching vibrations of C-H bonds in CH_4 molecules, the middle-frequency modes in the range of 1187–1402 cm^{-1} derive from the bending vibrations of C-H bonds in CH_4 molecules. The vibration modes of Mg atoms are all localized in the low-frequency region of 0–300 cm^{-1}. In the frequency region of 0–1025 cm^{-1}, the CH_4 molecular vibrations contribute most of phonon modes, which mainly results from the couplings between CH_4 and CH_4 and between CH_4 and Mg. For AlC_2H_8 at 80 GPa, the pressure makes H phonons shift towards higher frequency and enable phonon band broadening. The stretching vibration of C-H bonds in CH_4 makes phonon in the frequency region 2466–2715 cm^{-1}. The bending modes from C-H bonds distribute in the bigger frequency region of 831–1413 cm^{-1}. However, the pressure makes CH_4 molecular vibrations weak, narrowing the frequency to a small range of 0–830 cm^{-1}.

Combining electronic with phonon states, the electron-phonon interactions were analyzed by calculating the Eliashberg spectral function $\alpha^2 F(\omega)$. Then, the electron-phonon coupling constant λ was obtained based on the $\alpha^2 F(\omega)$. As shown in Fig. 5, the total λ is 0.79 for MgC_2H_8 at 40 GPa and 1.01 for AlC_2H_8 at 80 GPa, respectively. In MgC_2H_8, the contribution of Mg (by charge transfer) to total λ is about 19%, the contribution of $CH_4 - CH_4$ coupling is about 29%, while the contribution of H atoms reaches 52%. In AlC_2H_8, as a comparison, the contribution of Al (by charge

transfer) to total λ is about 29%, the contribution of $CH_4 - CH_4$ coupling is about 20%, the contribution of H atoms is still more than 51%. From these results, hydrogen dominates the electron-phonon coupling interaction in MC_2H_8, not carbon, which is similar to KB_2H_8, $MgCH_4$ [8], and $Ba(CH_4)_3$ [18], while it is different from $Li(CH)_4$ [12], KCH_4 [10], and $BeCH_4$ [11]. For other MC_2H_8 systems with lower T_c, such as $NaCH_4$ and KCH_4, the contribution of H to total λ is obviously less than 50%, which for $GaCH_4$ with high T_c, the contribution of H to total λ reaches 52%, also more than 50% (see Fig. S15 [43]). By comparing the T_c with λ values of these ternary hydrides, we can conclude that increasing the contribution of H to electron-phonon coupling is a way to design materials with high T_c.

IV. CONCLUSION

In summary, for $Fm\bar{3}m - MC_2H_8$ (M = K, Mg, Na, Al, and Ga), we have investigated their crystal structures, electronic states, phonon spectra, and electron-phonon interactions at selected low pressures based on the density functional theory and density functional perturbation theory. The metallization and possible superconductivity were analyzed. We found that MC_2H_8 maintains the molecular crystal characteristics, with a strong coupling between the C-H covalent bonds, while the metallization can be achieved by doping at selected low pressures. The absence of imaginary frequency in the calculated phonon spectra suggests that this MC_2H_8 structure is dynamically stable. The electron-phonon coupling

calculations reveal that NaC_2H_8, KC_2H_8, MgC_2H_8, AlC_2H_8, and GaC_2H_8 are all good BCS superconductors. Especially, the T_c of MgC_2H_8 can increase to 55 K at 40 GPa from 13.4 K at 20 GPa, and the T_c of AlC_2H_8 can reach 67 K at 80 GPa. Electronic states, phonon spectra, and the integral to Eliashberg spectral function show that H has a considerable contribution to the electron-phonon interaction in MgC_2H_8, AlC_2H_8, and GaC_2H_8 superconductors and indicate that increasing the contribution of H to electron-phonon coupling is a way to design materials with high T_c.

[1] A. P. Drozdov, M. I. Eremets, I. A. Troyan, V. Ksenofontov, and S. I. Shylin, Nature (London) **525**, 73 (2015).

[2] A. P. Drozdov, P. P. Kong, V. S. Minkov, S. P. Besedin, M. A. Kuzovnikov, S. Mozaffari, L. Balicas, F. F. Balakirev, D. E. Graf, V. B. Prakapenka, E. Greenberg, D. A. Knyazev, M. Tkacz, and M. I. Eremets, Nature (London) **569**, 528 (2019).

[3] M. Somayazulu, M. Ahart, A. K. Mishra, Z. M. Geballe, M. Baldini, Y. Meng, V. V. Struzhkin, and R. J. Hemley, Phys. Rev. Lett. **122**, 027001 (2019).

[4] E. Snider, N. Dasenbrock-Gammon, R. McBride, X. Wang, N. Meyers, K. V. Lawler, E. Zurek, A. Salamat, and R. P. Dias, Phys. Rev. Lett. **126**, 117003 (2021).

[5] P. Kong, V. S. Minkov, M. A. Kuzovnikov, A. P. Drozdov, S. P. Besedin, S. Mozaffari, L. Balicas, F. F. Balakirev, V. B. Prakapenka, S. Chariton, D. A. Knyazev, E. Greenberg, and M. I. Eremets, Nat. Commun. **12**, 5075 (2021).

[6] I. A. Troyan, D. V. Semenok, A. G. Kvashnin, A. V. Sadakov, O. A. Sobolevskiy, V. M. Pudalov, A. G. Ivanova, V. B. Prakapenka, E. Greenberg, A. G. Gavriliuk, I. S. Lyubutin, V. V. Struzhkin, A. Bergara, I. Errea, R. Bianco, M. Calandra, F. Mauri, L. Monacelli, R. Akashi, and A. R. Oganov, Adv. Mater. **33**, 2006832 (2021).

[7] M. Gao, X.-W. Yan, Z.-Y. Lu, and T. Xiang, Phys. Rev. B **104**, L100504 (2021).

[8] F. Tian, D. Li, D. Duan, X. Sha, Y. Liu, T. Yang, B. Liu, and T. Cui, Mater. Res. Express **2**, 046001 (2015).

[9] C. Kokail, W. von der Linden, and L. Boeri, Phys. Rev. Mater. **1**, 074803 (2017).

[10] J.-X. Han, H. Zhang, and G.-H. Zhong, Int. J. Mod. Phys. C **30**, 1950061 (2019).

[11] H.-Y. Lv, S.-Y. Zhang, M.-H. Li, Y.-L. Hai, N. Lu, W.-J. Li, and G.-H. Zhong, Phys. Chem. Chem. Phys. **22**, 1069 (2020).

[12] N. Lu, Y.-L. Hai, H.-Y. Lv, W.-J. Li, C.-L. Yang, and G.-H. Zhong, Int. J. Mod. Phys. C **32**, 2150032 (2021).

[13] S. Di Cataldo, C. Heil, W. von der Linden, and L. Boeri, Phys. Rev. B **104**, L020511 (2021).

[14] X. Liang, A. Bergara, X. Wei, X. Song, L. Wang, R. Sun, H. Liu, R. J. Hemley, L. Wang, G. Gao, and Y. Tian, Phys. Rev. B **104**, 134501 (2021).

[15] A. P. Durajski and R. Szczesniak, Phys. Chem. Chem. Phys. **23**, 25070 (2021).

[16] W.-H. Yang, W.-C. Lu, W. Qin, H.-J. Sun, X.-Y. Xue, K. M. Ho, and C. Z. Wang, Phys. Rev. B **104**, 174106 (2021).

[17] R. Lucrezi, S. Di Cataldo, W. von der Linden, L. Boeri, and C. Heil, arXiv:2112.02131.

[18] M.-J. Jiang, H.-L. Tian, Y.-L. Hai, N. Lu, P.-F. Tong, S.-Y. Wu, W.-J. Li, C.-L. Yang, and G.-H. Zhong, ACS Appl. Electron. Mater. **3**, 4172 (2021).

[19] G. Kresse and J. Furthmuller, Comput. Mater. Sci. **6**, 15 (1996).

[20] G. Kresse and J. Furthmuller, Phys. Rev. B **54**, 11169 (1996).

[21] J. P. Perdew, K. Burke, and M. Ernzerhof, Phys. Rev. Lett. **77**, 3865 (1996).

[22] G. Kresse and D. Joubert, Phys. Rev. B **59**, 1758 (1999).

[23] P. Giannozzi, S. Baroni, N. Bonini, M. Calandra, R. Car, C. Cavazzoni, D. Ceresoli, G. L. Chiarotti, M. Cococcioni, I. Dabo, A. Dal Corso, S. Fabris, G. Fratesi, S. de Gironcoli, R. Gebauer, U. Gerstmann, C. Gougoussis, A. Kokalj, M. Lazzeri et al., J. Phys.: Condens. Matter **21**, 395502 (2009).

[24] P. Giannozzi, O. Andreussi, T. Brumme, O. Bunau, M. B. Nardelli, M. Calandra, R. Car, C. Cavazzoni, D. Ceresoli, M. Cococcioni, N. Colonna, I. Carnimeo, A. Dal Corso, S. de Gironcoli, P. Delugas, R. A. DiStasio, Jr, A. Ferretti, A. Floris, G. Fratesi, G. Fugallo et al., J. Phys.: Condens. Matter **29**, 465901 (2017).

[25] P. B. Allen and R. C. Dynes, Phys. Rev. B **12**, 905 (1975).

[26] C. S. Barrett, Acta Crystallogr. **9**, 671 (1956).

[27] A. Jain, S. P. Ong, G. Hautier, W. Chen, W. D. Richards, S. Dacek, S. Cholia, D. Gunter, D. Skinner, G. Ceder, and K. A. Persson, APL Mater. **1**, 011002 (2013).

[28] K.-H. Klöss, D. Hinz-Hübner, and U. Ruschewitz, Z. Anorg. Allg. Chem. **628**, 2701 (2002).

[29] L.-G. Liu, J. Phys. Chem. Solids **47**, 1067 (1986).

[30] A. Simon, W. Bramer, B. Hillenkoetter, and H. J. Kullmann, Z. Anorg. Allg. Chem. **419**, 253 (1976).

[31] H. Föeppl, Angew. Chem. **70**, 401 (1958).

[32] M. Fatmi, B. Ghebouli, M. A. Ghebouli, A. Bouhemadou, and S. Binomran, J. Phys. Chem. Solids **73**, 1 (2012).

[33] P. Li, G. Gao, Y. Wang, and Y. Ma, J. Phys. Chem. C **114**, 21745 (2010).

[34] P. Karen, A. Kjekshus, Q. Huang, and V. L. Karen, J. Alloys Compd. **282**, 72 (1999).

[35] D. Moser, D. J. Bull, T. Sato, D. Noréus, D. Kyoi, T. Sakai, N. Kitamura, H. Yusa, T. Taniguchi, W. P. Kalisvaart, and P. Notten, J. Mater. Chem. **19**, 8150 (2009).

[36] A. Zoroddu, F. Bernardini, P. Ruggerone, and V. Fiorentini, Phys. Rev. B **64**, 045208 (2001).

[37] P. Vajeeston, P. Ravindran, and H. Fjellvåg, J. Alloys Compd. **509**, S662 (2011).

[38] S. Sridharan and H. Nowotny, Int. J. Mater. Res. **74**, 468 (1983).

[39] M. de Koning, A. Antonelli, and D. A. C. Jara, Phys. Rev. B **80**, 045209 (2009).

[40] L. Bosio, J. Chem. Phys. **68**, 1221 (1978).

[41] A. S. Naumova, S. V. Lepeshkin, and A. R. Oganov, J. Phys. Chem. C **123**, 20497 (2019).

[42] C. J. Pickard and R. J. Needs, Nat. Phys. **3**, 473 (2007).

[43] See Supplemental Material at http://link.aps.org/supplemental/10.1103/PhysRevB.105.104511 for electronic density of states and phonon spectra of MC_2H_8 at selected pressures, total energy, and electronic structure change with respect to the rotation of CH_4 quasimolecules, the number of Fermi surface changing with the pressure, the DOS values at Fermi level for MC_2H_8 at different pressures, the calculated Eliashberg spectral function $\alpha^2 F(\omega)$, and electron-phonon coupling integral $\lambda(\omega)$ for NaC_2H_8 at 60 GPa, KC_2H_8 at 100 GPa, and GaC_2H_8 at 60 GPa, and structural parameters of MC_2H_8 in format of POSCAR files.

[44] M. Einaga, M. Sakata, T. Ishikawa, K. Shimizu, M. I. Eremets, A. P. Drozdov, I. A. Troyan, N. Hirao, and Y. Ohishi, Nat. Phys. **12**, 835 (2016).

[45] G. Henkelman, A. Arnaldsson, and H. Jónsson, Comput. Mater. Sci. **36**, 354 (2006).

[46] M. Yu and D. R. Trinkle, J. Chem. Phys. **134**, 064111 (2011).

[47] M. Martinez-Canales and A. Bergara, High Press. Res. **26**, 369 (2006).

[48] L. L. Sun, Z. X. Zhao, A. L. Ruoff, C. D. Zha, and G. Stupian, J. Phys.: Condens. Matter **19**, 425206 (2007).

[49] G. Gao, A. R. Oganov, Y. Ma, H. Wang, P. Li, Y. Li, T. Iitaka, and G. Zou, J. Chem. Phys. **133**, 144508 (2010).

[50] D. Duan, Y. Liu, F. Tian, D. Li, X. Huang, Z. Zhao, H. Yu, B. Liu, W. Tian, and T. Cui, Sci. Rep. **4**, 6968 (2015).

[51] H. Liu, I. I. Naumov, R. Hoffmann, N. W. Ashcroft, and R. J. Hemley, Proc. Natl. Acad. Sci. USA **114**, 6990 (2017).

[52] A. Anderson and R. Savoie, J. Chem. Phys. **43**, 3468 (1965).

[53] A. Cabana and N. D. Thé, Can. J. Chem. **55**, 3862 (1977).

[54] K. Kobashi, K. Okada, and T. Yamamoto, J. Chem. Phys. **66**, 5568 (1977).

[55] F. D. Medina and W. B. Daniels, J. Chem. Phys. **70**, 2688 (1979).

[56] F. D. Medina and W. B. Daniels, J. Chem. Phys. **70**, 242 (1979).

[57] D. Fabre, M. M. Thiéry, and K. Kobashi, J. Chem. Phys. **76**, 4817 (1982).

[58] G. Millot, B. Lavorel, and J. I. Steinfeld, J. Chem. Phys. **95**, 7938 (1991).